Published in final edited form as:
Int J Cancer. 2015 March 1; 136(5): 1095–1103. doi:10.1002/ijc.29093.

Fluorescence-Based Endoscopic Imaging of Thomsen-Friedenreich Antigen to Improve Early Detection of Colorectal Cancer

Shinji Sakuma[1,*], **James Y. H. Yu**[6], **Timothy Quang**[5], **Ken-Ichiro Hiwatari**[2], **Hironori Kumagai**[2], **Stephanie Kao**[6], **Alex Holt**[6], **Jalysa Erskind**[6], **Richard McClure**[6], **Michael Siuta**[6], **Tokio Kitamura**[1], **Etsuo Tobita**[2], **Seiji Koike**[2], **Kevin Wilson**[6], **Rebecca Richards-Kortum**[5], **Eric Liu**[4], **Kay Washington**[3], **Reed Omary**[6,7], **John C. Gore**[6,7,8,9,11,12], and **Wellington Pham**[6,7,8,9,10,11,*]

[1]Faculty of Pharmaceutical Sciences, Setsunan University

[2]Life Science Materials Laboratory, ADEKA Corp., Tokyo Japan

[3]Vanderbilt School of Medicine, Division of Gastrointestinal and Hepatic Pathology

[4]Vanderbit School of Medicine, Department of Surgery and Surgical Oncology

[5]Rice University, Department of Bioengineering

[6]Institute of Imaging Science

[7]Department of Radiology and Radiological Sciences

[8]Department of Biomedical Engineering

[9]Vanderbilt Ingram Cancer Center

[10]Vanderbilt Institute of Chemical Biology

[11]Vanderbilt Brain Institute

[12]Molecular Physiology and Biophysics

Abstract

Thomsen-Friedenreich (TF) antigen belongs to the mucin-type tumor-associated carbohydrate antigen. Notably, TF antigen is overexpressed in colorectal cancer (CRC) but is rarely expressed in normal colonic tissue. Increased TF antigen expression is associated with tumor invasion and metastasis. In this work, we sought to validate a novel nanobeacon for imaging TF-associated CRC in a preclinical animal model. We developed and characterized the nanobeacon for use with fluorescence colonoscopy. In vivo imaging was performed on an orthotopic rat model of colorectal cancer. Both white light and fluorescence colonoscopy methods were utilized to establish the ratio-imaging index for the probe. The nanobeacon exhibited specificity for TF-

[*]Main Correspondence to: Wellington Pham, PhD, Vanderbilt University School of Medicine, 1161, 21st Avenue South, Nashville, TN 37232-2310, Tel: (615) 936-7621, wellington.pham@vanderbilt.edu, Or, Shinji Sakuma, PhD, Setsunan University, 45-1 Nagaotoge-cho, Hirakata, Osaka 573-0101, Japan, Tel: 72-866-3124, sakuma@pharm.setsunan.ac.jp.

Disclosure of Potential Conflicts of Interest
No potential conflicts of interest were disclosure

associated cancer. Fluorescence colonoscopy using the probe can detect lesions at the stage which is not readily confirmed by conventional visualization methods. Further, the probe can report the dynamic change of TF expression as tumor regresses during chemotherapy.

Data from this work suggests that fluorescence colonoscopy can improve early CRC detection. Supplemented by the established ratio-imaging index, the probe can be used not only for early detection, but also for reporting tumor response during chemotherapy. Furthermore, since the data obtained through in vivo imaging confirmed that the probe was not absorbed by the colonic mucosa, no registered toxicity is associated with this nanobeacon. Taken together, these data demonstrate the potential of this novel probe for imaging TF antigen as a biomarker for the early detection and prediction of the progression of CRC at the molecular level.

Despite recent advances in chemotherapeutics, colorectal cancer (CRC) remains a major cause of morbidity and mortality among cancers (1). Because CRC undergoes a protracted asymptomatic stage before it reaches the advanced stage, successfully detecting the early onset of the disease via routine screening will improve therapeutic outcomes and save lives. In that regard, colonoscopy is considered the gold standard for early detection. The process involves visual endoscopic inspection of the intestinal walls to detect polyps and adenomas. However, its effectiveness in the early detection of tumor growth is mitigated by its inability to disclose changes at the molecular level. For that reason, colonoscopy is ill suited for the assessment of tumors with a diameter of less than one centimeter (2). Recent studies have reported that the miss rate for this size-dependent technique may be as high as 20% for polyps (3). Additionally, those reports suggest that early detection of CRC is a far more difficult task than previously thought. Since in many cases, small or flat adenomas which are ten times more likely to become malignant than similarly sized polyps, are virtually indistinguishable from their surrounding tissue based on visual inspection alone (4). Further, colonoscopy lacks the capacity to detect cancer at the molecular level, thus leaving clinicians with no reliable metric capable of helping them determine whether a lesion is benign or malignant. These drawbacks have necessitated the development of novel technologies to achieve the early detection of CRC. One of the approaches is the integration of colonoscopy with an optical imaging modality. This innovation provides a robust method for early detection of CRC owing to its intrinsic coupling of detection with the underlying molecular-level pathology of the disease. Moreover, since molecular imaging methods can detect functional variations in tissue as opposed to changes in structure, they have the ability to focally highlight lesions with very high target-to-background ratios (5). Kelly et al. (6) demonstrated this notion using specific peptides that were identified through differential phase displays. In this work, the fluorescence (FL)-labeled peptide could detect CRC even when the cancer was limited to the submucosal layer using FL colonoscopy. In a similar approach, Hsiung et al (7) reported the use of phage display to develop a specific peptide capable of recognizing dysplastic colonocytes. After labeling the peptides with Fluorescein, the topically applied reporter can detect dysplastic colonoctyes with 81% sensitivity and 82% specificity using confocal microendoscopy.

In a different approach, we integrate nanotechnology with molecular imaging to develop a multiplex nanobeacon with which to image CRC using FL microendoscopy. The nanobeacon was coated with peanut agglutinin (PNA) on the surface as the recognition

molecules to recognize Thomsen-Friedenreich (TF) antigen (Galβ1, 3GalNacα-O-Ser/Thr) expressed in CRC. Different from other colon cancer imaging targets that require targeting agents to remain intact through systemic delivery, TF expression is found on the surface of epithelial cells; thus localized, topical delivery can be implemented to improve the efficiency of the targeting agents. Further, TF's substantially large size and accessibility at the cell surface coupled with the occurrence of tandem repeated regions (most TF disaccharides are expressed on the tandem repeated MUC protein backbone) help amplify the targeting signal. Based on these results, it seems reasonably certain that high expression of TF antigen in CRC combined with its absence from normal tissue represents a unique association in colorectal carcinoma that exhibits the qualities of a prognostic biomarker.

In this study, we report the validation of the specificity of the nanobeacon developed in our laboratory (Fig. 1). In addition to the presence of PNA on the surface, the nanobeacon is comprised of a polystyrene core encapsulated coumarin 6 dyes within its central core. The surface was coated with a thin layer of two polymers, poly(methacrylic acid) (PMAA) and poly(N-vinyl acetamide) (PNVA). Here, the former is used to attach the PNA through covalent bonding while the latter helps reduce nonspecific interaction with the mucous layer of the gastrointestinal tract (8, 9). In the recent past, we demonstrated the specificity of the nanobeacon in vitro using human CRC cells and biopsy specimens (10). The data obtained from that work showed that the nanobeacon can report the dynamic expression of TF antigen in CRC cells and tissues. In the current work, we demonstrated for the first time the in vivo imaging of TF-associated CRC using the nanobeacon along with an in-house developed FL microendoscope. Employing this imaging system, our in vivo imaging data not only confirms our previous reports of the nanobeacon's specificity for TF antigen (10–12), but additionally expands our findings by demonstrating that the nanobeacon can detect CRC weeks before the tumor can be visualized by white light (WL) colonoscopy. Furthermore, by using a standardized regional FL ratio imaging approach, we generated a ratio-imaging index (RII) for the nanobeacon. Using this approach, we demonstrated that the nanobeacon can be used in conjunction with colonoscopic imaging to provide early detection and assess tumor response to chemotherapy.

MATERIALS AND METHODS

Reagents

Cell culture mediums were obtained commercially at high grade, while the anti-human TF monoclonal antibody was obtained from Lifespan Biosciences. Immunohistochemical staining for colorectal section samples was performed using the avidin-biotin peroxidase complex method available in a commercial kit (Vector laboratories).

Nanobeacon synthesis and characterization

The synthesis of the nanobeacon was described in our recent publication (10) but accomplished here with major modifications aiming for in vivo and clinical applications (Supplementary data).

To estimate the encapsulation properties of coumarin 6, FL nanospheres with only surface PNVA chains were prepared at a different concentration of the dye during the copolymerization. Vinylbenzyl group-terminated PNVA (1.0 g) and styrene (1.0 g) were dissolved in 15 mL of the ethanol/water mixture containing AIBME (approximately 1 mol% of the total monomers) and coumarin 6 (0.1 – 1% of the total monomers). The nanospheres were prepared in the same manner as that described in the previous paragraph. PNA molecules were covalently conjugated on the surface of the nanobeacon through the coupling of the amino groups of PNA with the carboxyl groups of PMAA using 1-ethyl-3-(3–dimethylaminopropyl) carbodiimide as a catalyst. The resulting PNA-immobilized fluorescent nanospheres with surface PNVA chains were purified by changing the dispersion media several times. Finally, purified water was used in the filtration process to provide the nanobeacon solution at a concentration of 20 mg/mL.

The homogeneity and particle size were assessed via scanning electron microscopy (SEM) and dynamic light scattering (DLS). While the composition, quantity and thickness of the surface coating polymer were assessed using X-ray photoelectron spectroscopy (XPS). The amount of PNA was quantified by its hydrolysis from a known concentration of nanobeacon in the solution using hydrochloric acid. Under such conditions, PNA was also hydrolyzed into amino acids which were separated from the nanoparticles by active filtration. In addition, the weight amount of PNA relative to the concentration of the nanobeacon was quantified using adsorption isotherm approach where we examined several conditions of PNA immobilization with 10 mg of the nanobeacon. Afterward, the amount of the PNA immobilized on the nanobeacon was quantified by ninhydrin assay and compared to a calibrated PNA concentration curve. While the amount of coumarin 6 present in the nanobeacon was assessed using UV-Vis spectroscopy. Further, we used gel permeation chromatography (GPC) to quantify the distribution ratio of the polymers.

Cell line and animal models

Human HCT116 cells were maintained in Leibovitz's L15 with 1.5 mM McCoy's 5A. The medium was supplemented with fetal bovine serum (10%, v/v) and penicillin-streptomycin (100 U/mL).

Eight to ten-week-old female nude rats (rnu/rnu) were purchased from Harlan Laboratories. While wild type C57BL/6 mice were acquired from Jackson Laboratory. All experimental protocols were approved by the Vanderbilt University Institutional Animal Care and Use Committee.

To generate an orthotopic model of CRC, the lower abdominal region of isoflurane anesthetized female nude rats rnu/rnu (200 – 250 g) were sanitized with iodine prior to longitudinally incision (approximately 2 – 2.5 cm) with a surgical scalpel. The cecum was pulled out slightly and placed on a sterilized gauge to reveal the descending colon. Approximately, half a million HCT 116 cancer cells (10 μL) were injected into the submucosa of the descending colon. After injection, the descending colon and the cecum were returned to their normal positions and the wound closure was achieved in a double layer fashion using silk-based sutures. Tumor growth was monitored by FL and WL colonoscopy weekly until the tumors were detected at the earliest detectable time point.

White light colonoscopy

Visual examination of the colon before and after tumor implantation, and then at regular weekly intervals using an Olympus ENF-P4 endoscopic system (Olympus Optical Co.) equipped with a digital USB video camera (Image Pro Medit Inc.) and a 150 W halogen light source. The process began by inflating the colon of prone, isoflurane anesthetized mice using a modest stream (1.74 psi) of air (Air-1000, TopFin). The endoscope (diameter 3.4 mm) was inserted forward to the splenic flexure and was withdrawn slowly while capturing the video. The colonic epithelial tissues were examined via a monitor, and the data was captured as video and photos.

Fluorescence colonoscopy

Immediately following WL colonoscopy, the animals were subjected to FL colonoscopy. The nanobeacon was topically applied to the mucosa using a 360-degree spray catheter (Hobbs Medical Inc.). Thirty minutes following nanobeacon application, the probe was removed completely by suctioning using a syringe. Excess materials were completely removed by additional spraying of the colon with washing solution, such as PBS. FL colonoscopy was performed using a high-resolution and custom-built epi-fluoresecence microendscope to acquire in vivo imaging data. The system is comprised of a compact CCD camera (Point Grey Research), a high-power light emitting diodes (Luxeon) and micro fiber-optic bundles (Fujikura). The spatial resolution of the microendoscope was achieved using a gradient index lens assembled to the distal tip of the fiber bundle. The configuration of the optics is aligned so that the tip of the fiber bundle is imaged onto the tissue surface with demagnification, thereby increasing the spatial sampling frequency imposed by the light-guiding cores of the fiber bundle. The degree of demagnification corresponds to the increase in spatial resolution. All data were collected using coumarin 6- or RFP-compatible excitation/emission dichroic filters, and a fiber optics with a diameter of 600 μm which provides an overall optical resolution of 0.4 μm (13).

The procedure commenced with the smooth insertion of the endoscope into the anus of the anesthetized rats/mice. The endoscope could survey the large intestine all the way to the splenic flexure. Recording of the imaging data began as the endoscope was slowly withdrawn.

Standardized Regional Fluorescence Ratio imaging

The large intestine was virtually segmented into two regions in which the splenic flexure of the animal was considered a control tissue; as this region provides an anatomically fixed reference that could be reliably located between imaging sessions. Measurements of the FL signal at the splenic flexure were taken before and after application of the nanobeacon in the descending colon. The pretreatment and posttreatment signals were then averaged and used as F_0 – an index of non-specific FL signal. The tumor-bearing region of the colon was defined as a region of interest (ROI) and measurements of the FL signal emanating from this area were averaged and defined as F_{ROI} – an index of tumor specific FL. The F_{ROI}/F_0 ratio was then established by averaging the data values determined from 6 tumor-bearing animals.

Quantitative analysis

Quantitative analysis of FL colonoscopy luminance was conducted using the MATLAB software package (MathWorks, Inc., USA). Data from each colonoscopy image was initially combined to automatically create a global threshold level using Otsu's method (14). This threshold was applied to each image to create binary images representing dark and bright pixels. Percentages of overall bright pixels in each image are presented. While RGB images of TF histology were analyzed and segmented into pixels where intensities of the brown color were analyzed and presented as percentages of overall brown dominated pixels in each slide.

Immunohistochemistry

The freshly isolated descending colons of the rats were removed, fixed in 4% paraformaldehyde, embedded in OCT and frozen, after which section slides were prepared. Slide sections were stained with TF monoclonal antibodies using the avidin-biotin peroxidase complex method available in a commercial kit (Vectastain ABC Elite Kit, Vector Laboratories, USA) and analyzed by WL microscopy.

Statistical analysis

Data were analyzed using GraphPad software (GraphPad Prism version 4.0 for Mac). Results are presented as mean ± SE. Differences were analyzed with student's t-test for two-factor ANOVA, and the results are considered significant at a P value of <0.05.

RESULTS

Specificity and quantitative analysis of the components makeup of the nanobeacon

Homogeneity, particle size and the FL property of the nanobeacon were assessed using SEM and FL microscopy. As shown in Fig. 2 A and B, the nanobeacon is homogenous in size and shape. The FL signal emitted from the nanobeacon is uniform, which suggests equal distribution of coumarin 6 dye within the particle's central core. The specificity of the nanobeacon was confirmed by incubation with HCT-116 cells (Fig. 2 C). Of note, restriction of the FL signal to the cell rim corroborates with the notion that TF expression is predominately located in the extracellular membrane. This interpretation of the data is also supported by information obtained by high-resolution confocal microscopy, which again demonstrates that the nanobeacon, and thus TF expression, are restricted to the extracellular membrane (Supplementary Fig. S1). To assess the level of non-specific binding between the nanobeacon and endogenous cell-surface antigens, the nanobeacon was incubated in a TF-deficient batch of cells. In this experiment, TF expression was depleted from the cell surface via treatment with glycanase using the procedures described by Singh et al. (15). Using this method, the TF antigen removal on the cell surface was quantified by cell sorting analysis. We confirmed that more than 50% of the antigen was depleted upon an overnight exposure to the enzyme (Supplementary Fig. S2). Following TF depletion, the cells were again incubated with the nanobeacon and analyzed for FL signal. As shown in Fig. 2 D, removal of TF from the surface of CRC cells resulted in a profound attenuation of FL signal. This

data supports the conclusion that binding of the nanobeacon to the cell surface is TF-dependent.

To further characterize the nanobeacon's physical property, the composition, quantity and thickness of the surface coating polymer were assessed using XPS. As shown in Table 1, polystyrene accounts for the majority of the nanobeacon, and its surface is coated with PNVA and PMAA at a thickness of approximately 15 nm. To facilitate the quantification of PNA associated with each nanoparticle, PNA was quantified in its hydrolyzed form. We found that 200–300 PNA molecules had been covalently linked on each nanobeacon particle. Furthermore, using an adsorption isotherm technique, we learned that quantitatively there are about 2 μg of PNA for every 1 mg/mL of the nanobeacon (supplementary Fig. S3). In addition, we found that coumarin 6 dye constitutes approximately 0.05% of the nanobeacon's overall weight. Overall, the nanobeacon ranges from 300,000–1,500,000 daltons, which is equivalent to 350 nm. Most importantly, we can control the size of the nanobeacon by varying polymer ratios during the synthesis. However, it is crucial to maintain the size above 300 nm to prevent the nanobeacon from being absorbed by the intestinal mucosa and subsequently becoming toxic to the peripheral organs due to systemic distribution (10).

Topically applied nanobeacon is nonabsorbable by colonic epithelial tissue

As mentioned earlier, we performed the biodistribuiton of the nanobeacon using an orthotopic mouse model in the past (10). In that work we found out that the nanobeacon was not absorbed by the colonic mucosa. In this work, we want to further confirm that notion by imaging using FL colonoscopy. Three groups of wild-type mice (n=6, each) were treated with (i) saline; (ii) coumarin 6 dye or (iii) nanobeacon. As shown in Fig. 3 A, the FL signal emitted by the nanobeacon-treated animals was comparable with that of mice treated with saline. This result supports the conclusion that the nanobeacon exhibits negligible non-specific interaction with endogenous antigens and that retention after washing is dependent on TF expression. In contrast, the coumarin 6 dye readily diffused through the mucosa and produced an enhanced FL signal which depicted the colonic crypts of the descending colon.

Ratio-imaging index

In this task, we developed a ratio imaging method which enabled us to create an imaging index specific to the nanobeacon. This standardized metric is useful for enhancing the probe's precision and reproducibility relative to its cancer prediction capability. To generate a RII for each value of F_0 and F_{ROI}, we averaged the data obtained from 6 orthotopic CRC rats. For a nanobeacon concentration of 2 mg/mL, the RII of the nanobeacon F_{ROI}/F_0 was determined to be 1.3 (Table 2). Using this index, we hypothesized that an RII value derived from any screening subject larger or equal to 1.3 could be characterized as cancer suspect. Subsequent in vivo imaging using this parameter demonstrated that an RII of 1.3 represents the threshold for early CRC detection. The results of this analysis suggest that the nanobeacon binds to CRC tissue with greater avidity compared to a noncancerous area. The mean signal intensity in the tumor region was significantly higher compared to the untreated control splenic flexure.

The nanobeacon leverages colonoscopy for early CRC detection

Using the established RII, we were able to distinguish TF-associated CRC from normal colonic tissue in vivo. The advantage of this approach is that it is both practical and clinically relevant because we can utilize the FL signal emitted by the nanobeacon for direct diagnosis without the need to perform imaging on control subjects. As shown in Fig. 3 B, four weeks after tumor induction, FL colonoscopy assisted by the nanobeacon (2 mg/mL) detected the tumor with an RII index above 1.3 ($p<0.001$). Quantitatively, the FL signal of this early stage CRC was 52-fold higher than that of the control tissue ($p<0.05$) (Fig. 3 C), an observation confirmed by IHC data. The intensity of TF-stained CRC specimens was 35-fold higher than the control ($p<0.05$). Altogether, it became apparent that at the early stage of tumor development, WL colonoscopy was not sufficient to enable a decision despite or observation of an irregular surface pattern on the gastric mucosa. However, FL colonoscopy data detected the TF expression and reported CRC with certainty.

Six weeks after injecting the cells into another group of animals, the resultant tumors were large enough to be detected by WL colonoscopy. As the tumors grew, TF expression became more prominent (16). Therefore, the FL signal that resulted from binding the nanobeacon to the TF-associated tumor increased markedly. Quantitative analysis of TF expression from FL colonoscopy imaging corroborates with IHC data. This suggests that TF expression is statistically significant in CRC compared to normal tissue and that the RII is approximately 1.5 ($p<0.05$) (Fig. 3 C). At this stage, the FL signal of the tumor was more than 60-fold higher compared to the control ($p< 0.05$). Likewise, the level of TF expression has a significant relation to the reported FL signal obtained from colonoscopy and was more than 60-fold different from the dissected tumor compared to the control tissue ($p<0.05$).

The nanobeacon can be used to distinguish tumor grade and report tumor response to chemotherapy

Having demonstrated that the nanobeacon can detect tumors with specificity, next we investigated whether nanobeacon-mediated detection of TF antigen correlated with tumor size. We designed two cohorts of animals ($n = 9$, each). One of these cohorts was the orthotopic model of CRC where nude rats were induced with HCT-116 CRC cells to generate TF-specific tumor in the descending colon. The second cohort was comprised of control animals in which no tumor model was invoked. FL colonoscopy was performed on both groups of animals and RII values were obtained. We graded the tumor using the criteria such that a grade 0 tumor indicated that WL colonoscopy could detect structural anomalies of the epithelial lining. However, at this stage WL imaging alone could not reliably detect the presence of the tumor. A grade 1 tumor was defined such that it might be comparable to a small but the adenocarcinoma was reliably detectable by WL colonoscopy. While a grade 2 tumor was defined as those in which the tumor size reached approximately 1/8 of the diameter of the colon. As shown in Fig. 4 A, the RII values increased significantly at the threshold between the control and early CRC tissue. However, the FL signal began to level off as tumor size increased. This characteristic implies that the probe is suitable for early diagnosis applications. When we compared tumor size to the control for each group of tumor grades, the enhanced FL signal intensity was clear and statistically different from the control ($P<0.01$).

Having established the detection threshold, we then focused on validating if the nanobeacon could detect the dynamic change of TF expression during chemotherapy. Selected animals that had grade 2 tumors were treated with paclitaxel during a one-month therapy regiment that included 4 paclitaxel treatments (10 mg/kg via tail vein injection) (Fig. 4 B). Colonoscopies were performed immediately following and 30 days after the first treatment. At the beginning of the therapy, the tumor was apparent, and FL colonoscopy detected dense, abnormal and asymmetric crypts in the descending colon. The FL signal was above the 1.3 detection threshold. Biopsy samples stained with antibodies to the TF antigen also reported similar observation as seen in the FL colonoscopy, such that an increase was noted in the number of asymmetric crypts in which the TF antigen was overexpressed. At the end of the therapy period, the tumor was not detected by either WL or FL colonoscopy. The animals were sacrificed, the descending colon dissected and tumor regression confirmed by visual examination (data not shown). Histology confirmed that the colon was free of tumors. Taken together, this data suggests that the nanobeacon exhibits the potential for imaging tumor response during chemotherapy.

DISCUSSION

For imaging surface CRC biomarkers, the TF antigen continues to receive a remarkable amount of attention. Not only is the antigen overexpressed exclusively in CRC, but it is also carried by MUC1 on the apical surface of the colonic mucosa (17). Therefore, the antigen represents a unique target for topically applied molecular imaging probes. Although topical probes have been developed in the past for use in CRC imaging (7), we believe this is the first time a topical FL nanoparticle probe has been designed specifically for that purpose. Notably, the probe was alienated from the blood circulation, thus, reducing the potential of toxicity. In the recent past, we demonstrated that the nanobeacon was not incorporated into the systemic distribution process upon topical application using an orthotopic mouse model (10). That data verified that there was no detectable FL signal in the serum or other organs of an orthotopic mouse model several hours after applying the nanobeacon to the colon. In the current study, we hypothesize that FL colonoscopy can also be used to assess the distribution of the topical nanobeacon. As the TF antigen is absent from normal colonic tissue, applying the nanobeacon to the colon of control animals would not yield FL signals. Further, if the nanobeacon is not absorbed by the mucosa, then no FL signals should exist. As shown in Fig. 3 A, treatment of the nanobeacon on the normal colon emits a background FL signal as low as that of the saline-treated counterparts. Our observation corresponds with a report by Jani et al., who used I^{125}-labeled polystyrene nanoparticles to study absorption across the gastrointestinal tract. Their work showed that following the topical application of 300 nm-polystyrene microspherers to the rat intestines, they were not absorbed by the colonic mucosa and thus were completely absent in the blood (18).

Next, we wanted to determine whether the nanobeacon is capable of detecting TF-associated CRC at the early stage. To that end, we developed a novel orthotopic CRC rat model to assess the specificity of the nanobeacon. While orthotopic CRC tumors have been reported in the literature (6, 19, 20), no such models have yet been developed on rats. In this model, we implanted human CRC cells in the colonic submucosa using an open surgical method. Different from the subcutaneous model, rats were injected with fast-growing and highly

aggressive cancer cells, such as HCT-116; however, that did not guarantee robust tumor growth. Injection of the same amount of cells (5.0×10^5) in subcutaneous and submucosal models resulted in a very different tumor growth kinetic (Supplementary Fig. S4). Tumors in the subcutaneous model grew faster, which resulted in a mass effect within days rather than weeks. In the orthotopic model, the apparent HCT-116 CRC was detected by visual inspection after ten weeks of tumor induction. Tumors implanted orthotopically in rats are very similar to those that affect humans, since once formed in the colon, the tumors invade the colonic submucosa and latter progress to the serosa. The earliest time at which we can detect the early onset of the disease is approximately four weeks post cell injection using WL colonoscopy. While the small lesion was not obvious and did not prove sufficiently informative to help render a categorical decision regarding the presence of CRC, the nanobeacon demonstrated the ability to detect such molecular transformation. In fact, when we sprayed the colon with the nanobeacon, we noted a remarkably high FL signal at the suspected area. As shown in Fig. 3 B, these data suggest that the nanobeacon was retained in the lesion area and emitted a FL signal with an approximate F_{ROI}/F_0 index greater than 1.3. To correlate the imaging with biological events, the animals were sacrificed, after which the descending colons were collected for immunohistochemistry analysis. The results showed intense TF antigen staining in the colonic tissue of the lesions, particularly in the crypts, and that the antigen was certainly the driving force behind the PNA-derivatized nanobeacon binding.

During the course of work, we noted that the F_{ROI}/F_0 index increases as the tumor size increases. As demonstrated in Fig. 4 A, a large tumor has a F_{ROI}/F_0 index of 1.5 versus the 1.3 of an early-stage tumor. Since our strategy for using the nanobeacon is to leverage early detection, we are not interested in large tumors which can certainly be detected readily by WL colonoscopy. The relationship between tumor size and RII values suggests that there is a substantial difference in the index value between the control and early-stage tumors ($P<0.01$), and that difference maintains substantial between an early-stage tumor and a CRC grade 1 tumor. However, the gap narrowed between established tumors. Taken together, the data presented in the work suggested that the nanobeacon can be used not only for the early detection of CRC, but is also useful for reporting the response of cancer during chemotherapy.

In conclusion, we demonstrated the integration of nanotechnology with cancer imaging, an approach that offers several advantages that cannot be achieved by other methods. The nanobeacon can be used for the enhanced early detection and characterization of CRC, and it is suitable for screening colonoscopy. Further, preoperative endoscopic imaging can be helpful in localizing flat, small or subtle colonic lesions that may be difficult to identify by inspection during surgery. There remain a few important caveats; currently, little is known about the level of TF expression between endogenous flat adenocarcinoma and small tumor generated by injection of human carcinoma cells in the submucosa. Because the endogenous flat adenocarcinoma can proceed without major changes in cell surface glycosylation and this may undermine the application of the nanobeacon for early detection of CRC. To address this problem, we are attempting to test the nanobeacon on freshly dissected flat polyps. In addition, issues such as tissue autofluorescence due to the use of visible light need to be addressed in order to facilitate the technology for human use. Nevertheless, we

believe the development of a topically applied FL agent combined with extant imaging technologies make this project ideal for clinical translation.

Supplementary Material

Refer to Web version on PubMed Central for supplementary material.

Acknowledgements

The work was partially funded by R01 CA160700 (W.P.), P50 CA128323 (J. C. G.), R01 CA159178 (R.O.) from the NIH and the VICC Cancer Center Support grant (W.P.) and the Science Research Promotion Fund from The Promotion and Mutual Aid Corporation for Private Schools of Japan (2011–2012) (S.S.).

REFERENCES

1. Pisani P, Parkin DM, Bray F, Ferlay J. Estimates of the worldwide mortality from 25 cancers in 1990. Int J Cancer. 1999; 83:18–29. [PubMed: 10449602]
2. Siersema PD, Rastogi A, Leufkens AM, Akerman PA, Azzouzi K, Rothstein RI, et al. Retrograde-viewing device improves adenoma detection rate in colonoscopies for surveillance and diagnostic workup. World J Gastroenterol. 2012; 18:3400–3408. [PubMed: 22807609]
3. Aisenberg J. Gastrointestinal endoscopy nears "the molecular era". Gastrointest Endosc. 2008; 68:528–530. [PubMed: 18760179]
4. Jaramillo E, Watanabe M, Slezak P, Rubio C. Flat neoplastic lesions of the colon and rectum detected by high-resolution video endoscopy and chromoscopy. Gastrointest Endosc. 1995; 42:114–122. [PubMed: 7590045]
5. Sheth RA, Mahmood U. Optical molecular imaging and its emerging role in colorectal cancer. Am J Physiol Gastrointest Liver Physiol. 2010; 299:G807–G820. [PubMed: 20595618]
6. Kelly K, Alencar H, Funovics M, Mahmood U, Weissleder R. Detection of invasive colon cancer using a novel, targeted, library-derived fluorescent peptide. Cancer Res. 2004; 64:6247–6251. [PubMed: 15342411]
7. Hsiung PL, Hardy J, Friedland S, Soetikno R, Du CB, Wu AP, et al. Detection of colonic dysplasia in vivo using a targeted heptapeptide and confocal microendoscopy. Nat Med. 2008; 14:454–458. [PubMed: 18345013]
8. Sakuma S, Sudo R, Suzuki N, Kikuchi H, Akashi M, Hayashi M. Mucoadhesion of polystyrene nanoparticles having surface hydrophilic polymeric chains in the gastrointestinal tract. Int J Pharm. 1999; 177:161–172. [PubMed: 10205611]
9. Sakuma S, Sudo R, Suzuki N, Kikuchi H, Akashi M, Ishida Y, et al. Behavior of mucoadhesive nanoparticles having hydrophilic polymeric chains in the intestine. J Control Release. 2002; 81:281–290. [PubMed: 12044567]
10. Kumagai H, Pham W, Kataoka M, Hiwatari K, McBride J, Wilson KJ, et al. Multifunctional nanobeacon for imaging Thomsen-Friedenreich antigen-associated colorectal cancer. Int J Cancer. 2013; 132:2107–2117. [PubMed: 23055136]
11. Sakuma S, Higashino H, Oshitani H, Masaoka Y, Kataoka M, Yamashita S, et al. Essence of affinity and specificity of peanut agglutinin-immobilized fluorescent nanospheres with surface poly(N-vinylacetamide) chains for colorectal cancer. Eur J Pharm Biopharm. 2011; 79:537–543. [PubMed: 21693188]
12. Sakuma S, Kataoka M, Higashino H, Yano T, Masaoka Y, Yamashita S, et al. A potential of peanut agglutinin-immobilized fluorescent nanospheres as a safe candidate of diagnostic drugs for colonoscopy. Eur J Pharm Sci. 2011; 42:340–347. [PubMed: 21216286]
13. Pierce M, Yu D, Richards-Kortum R. High-resolution fiber-optic microendoscopy for in situ cellular imaging. J Vis Exp. 2011
14. Otsu N. A Threshold selection method from gray-level histogram. IEEE Transactions on Systems, Man, and Cybernetics. 1979; 9:62–66.

15. Singh R, Campbell BJ, Yu LG, Fernig DG, Milton JD, Goodlad RA, et al. Cell surfaceexpressed Thomsen-Friedenreich antigen in colon cancer is predominantly carried on high molecular weight splice variants of CD44. Glycobiology. 2001; 11:587–592. [PubMed: 11447138]

16. Yu LG. The oncofetal Thomsen-Friedenreich carbohydrate antigen in cancer progression. Glycoconjugate journal. 2007; 24:411–420. [PubMed: 17457671]

17. Brockhausen I. Mucin-type O-glycans in human colon and breast cancer: glycodynamics and functions. EMBO Rep. 2006; 7:599–604. [PubMed: 16741504]

18. Jani P, Halbert GW, Langridge J, Florence AT. Nanoparticle uptake by the rat gastrointestinal mucosa: quantitation and particle size dependency. The Journal of pharmacy and pharmacology. 1990; 42:821–826. [PubMed: 1983142]

19. Martin ES, Belmont PJ, Sinnamon MJ, Richard LG, Yuan J, Coffee EM, et al. Development of a colon cancer GEMM-derived orthotopic transplant model for drug discovery and validation. Clin Cancer Res. 2013; 19:2929–2940. [PubMed: 23403635]

20. Metildi CA, Kaushal S, Snyder CS, Hoffman RM, Bouvet M. Fluorescence-guided surgery of human colon cancer increases complete resection resulting in cures in an orthotopic nude mouse model. J Surg Res. 2013; 179:87–93. [PubMed: 23079571]

Novelty and Impact Statements

Thomsen-Friedenreich (TF) antigen is commonly present in cancer cells and in the colorectal mucous of patients with colorectal cancer. Biopsy samples taken from colorectal cancer patients showed that the TF antigen is overexpressed by hyperplastic and neoplastic colorectal cancers but not expressed in normal mucosa. In this work, we describe the development of a fluorescence nanoparticle for imaging TF antigen using fluorescence colonoscopy. The specificity of the probe was demonstrated in its ability to detect TF-associated colorectal cancer in the early stage, and the dynamic change of TF-based CRC during therapy. Based on these results, we hypothesize that the nanobeacon exhibits the qualities of a prognostic agent for detection colorectal cancer.

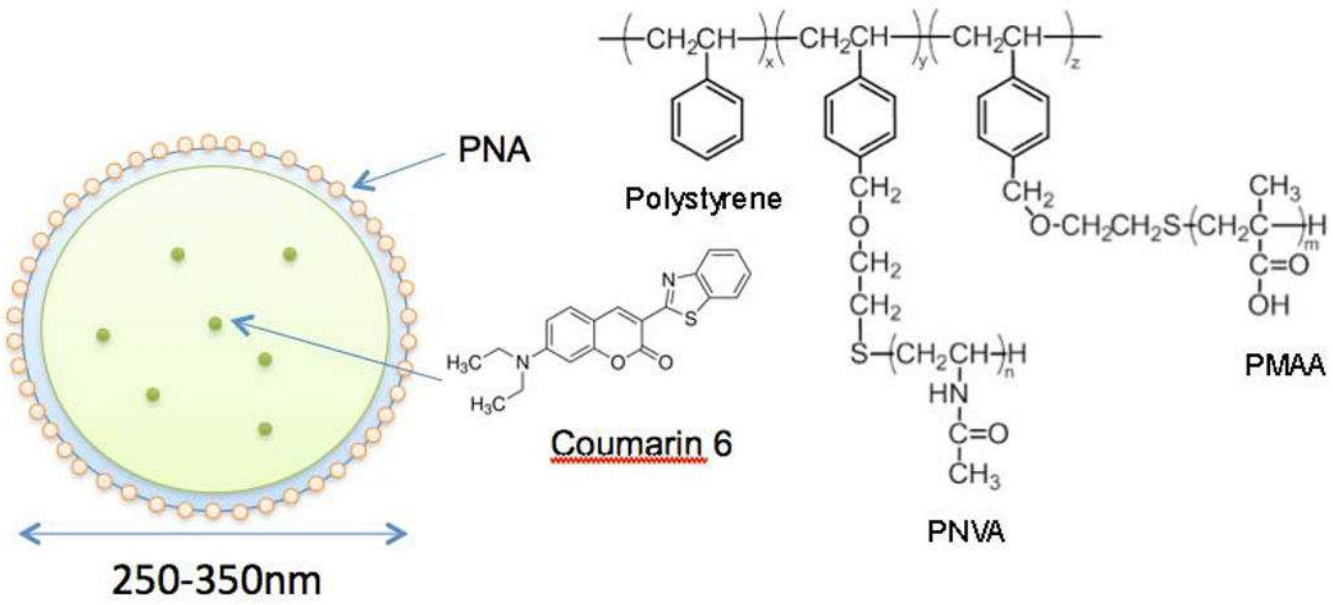

Figure 1.

Design and physical properties of the nanobeacon for FL colonoscopy. The nanobeacon is comprised largely of polystyrene polymer and its surface was coated with a thin layer of PNVA and PMAA polymers. The PNVA is employed to reduce nonspecific binding to normal colonic mucosa, while PMAA provides a handle for bioconjugation via carboxylic groups. Approximately 200–300 PNA moieties are attached to the nanobeacon through covalent bonding to the PMAA polymer as recognition molecules for TF antigen. The optical feature of the nanobeacon is provided by coumarin 6 dyes encapsulated within the core of the nanoparticle. Quantitatively, coumarin 6 dye constitutes approximately 0.05% of the overall weight of the nanobeacon.

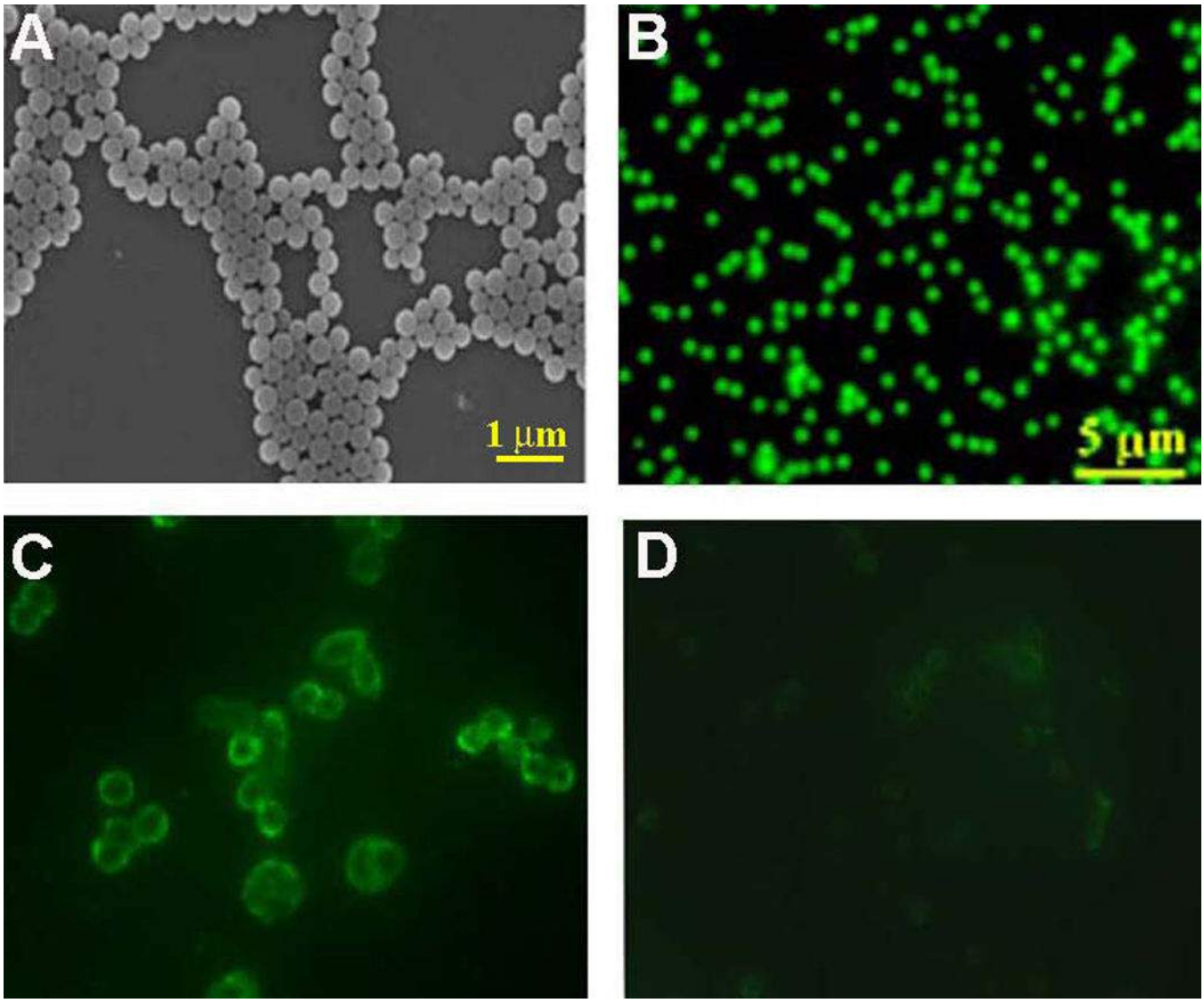

Figure 2.

Demonstration of the size, shape, optical characteristics and specificity of the nanobeacon. Homogeneity of the size, shape and fluorescence of the nanobeacon were confirmed by SEM (A) and FL microscopy (B), respectively. The specificity of the nanobeacon for TF antigen expressed on the surface of human CRC cells was tested on HCT-116 cells. Cells on chamber slides were treated with the nanobeacon (2 mg/mL) for 20 minutes in the incubator (25° C, 2% CO_2). Following incubation, the cells were washed twice with DPBS and observed via FL microscopy (C). The dynamically specific response of the nanobeacon was demonstrated in HCT-116 cells. In this work, the TF antigen resident on the surface of the cells was removed by glycanase before treating the cells with the nanobeacon (2 mg/mL). As a consequence of TF removal, the FL signal was weakened significantly (D). Exposure time in FL observation was 400 ms at a magnification of X 200 each.

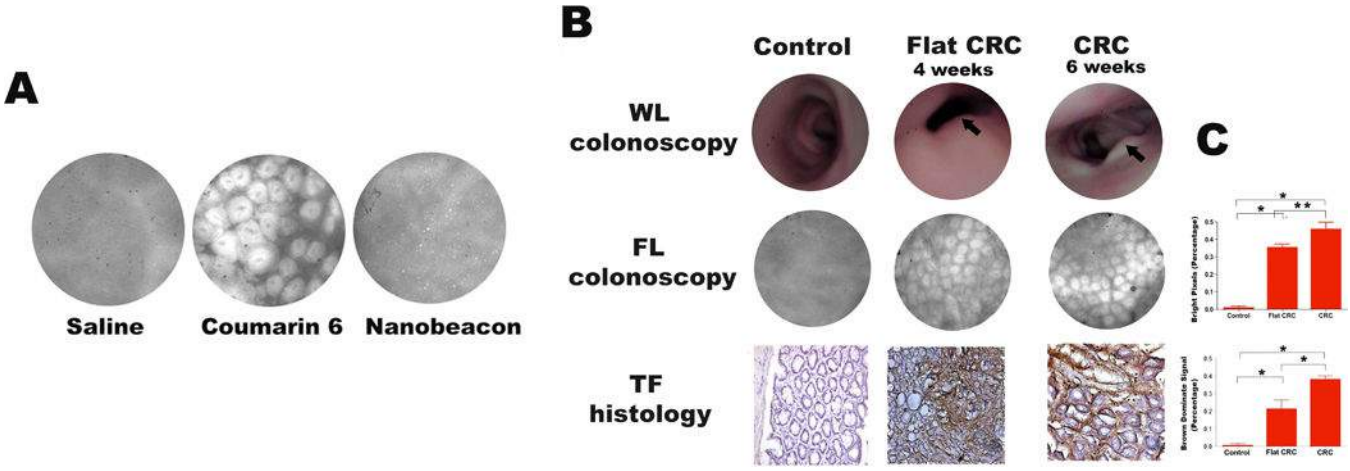

Figure 3.

(A) In vivo assessment of the biodistribution of the topically applied nanobeacon in wild-type mice. FL colonoscopy was performed after the colons of 3 cohorts of mice (n = 6, each) were treated for 30 minutes with saline, coumarin 6 dye or the nanobeacon delivered by a 360° spray catheter. (B) Representative images of WL versus FL colonoscopy for the early detection of CRC. Untreated control and HCT-116-induced rats, including those with early (4 weeks post-tumor cell injection, second column) and late (6 weeks post-tumor induction, third column) stage tumors (n = 6, each group) were screened by WL colonoscopy. The early-stage tumor (second column) was flat (grade 0), which impeded detection by WL visualization. In contrast, the result of ratio imaging using FL colonoscopy suggested that tissue anomaly could be CRC since the F_{ROI}/F_0 index > 1.3 ($p<0.001$, n = 18, three measurements per rat). After FL colonoscopy, tissue in the descending colon was collected for histology, and the data corroborates with that obtained from FL colonoscopy. In larger tumors (grade 2)(third column), both WL and FL colonoscopy can detect the lesion with a substantial level of confidence. As the tumor grew larger, TF expression became demonstrably higher than in smaller tumor. As a result, the ratio imaging F_{ROI}/F_0 index was >.5 ($P<0.05$, n = 18, three measurements per rat). (C) Quantification of the signal intensity emitted from the nanobeacon and histology data as a function of tumor size using Matlab analysis. Both techniques showed significantly increased signals in flat tumor (grade 0) compared to control. In additon, larger tumors exhibited stronger signals compared to smaller tumors. Data are presented as mean ± SE *, $P<0.05$; **, $P<0.001$.

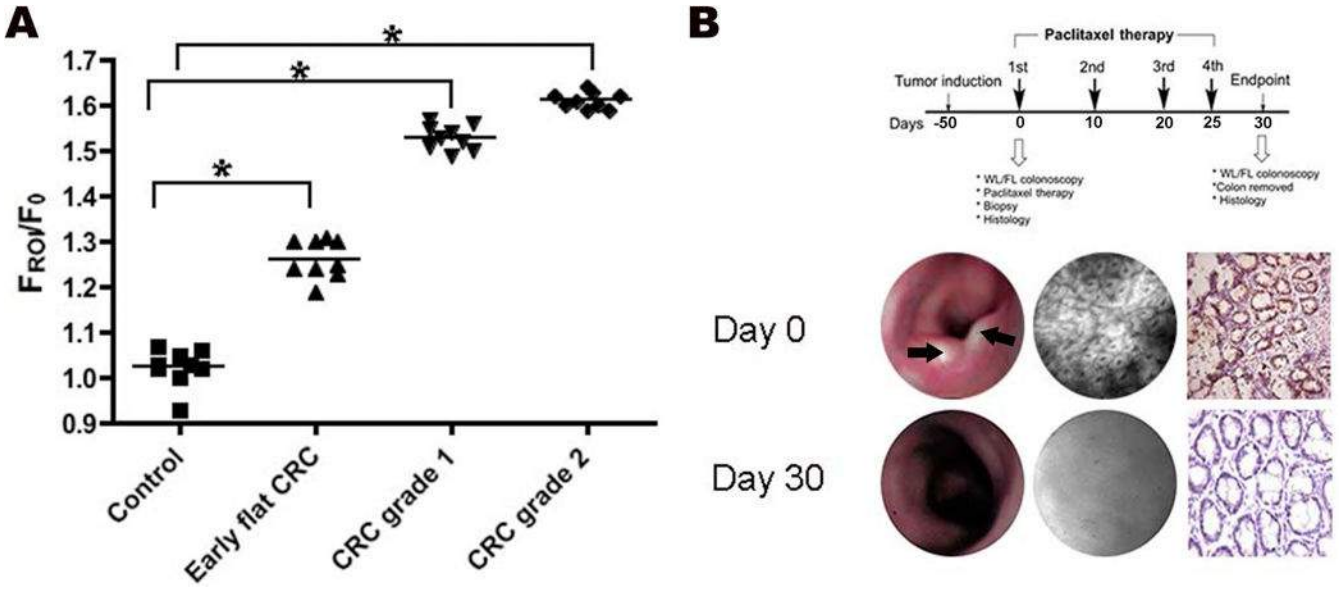

Figure 4.

(A) Correlation between the ratio imaging index F_{ROI}/F_0 with tumor size. Each data point represents the F_{ROI}/F_0 ratio of a single HCT-116-induced rat. The tumors were allowed to grow and their sizes were assessed using WL colonoscopy starting from grade 0 to grade 2. At each classified stage of tumor progression, statistically significant differences in F_{ROI}/F_0 were recorded ($P<0.01$). This result supports the conclusion that TF antigen expression increases with tumor progression and confirms the reliability of the nanobeacon to report this increase; (B) Nanobeacon and FL colonoscopy were able to report the dynamic change of TF antigen as the tumor regressed during chemotherapy. Grade 2 CRC-tumor bearing rats (n = 3) were treated with a high dosage regimen of paclitaxel (10 mg/Kg) over a period of approximately one month per the detailed treatment timeline. Prior to chemotherapy, stereotactically guided WL and FL colonoscopies were performed to determine the location of the suspected tumor. A tissue biopsy was performed at the location defined using a retractable needle to confirm CRC pathology. Upon completion of the treatment, WL and FL colonoscopies were performed prior to tissue collection for visual examination and histology.

Table 1

Overall physical property of the nanobeacon.

Physical properties	Actual Values	Techniques
Mw PMA:PNVA	12000±1000 : 8000±2000	GPC
Thickness of PMA/PNVA	15 nm	XPS, ^{1}HNMR
Ratio Styrene:PMA:PNVA	600 : 3 : 2	NMR
Mw Nanobeacon	300,000–1,500,000	GPC
Surface Fabricated PNA	2–4 μg/mg nanoparticle 200 – 300 PNA molecules	Adsorption Isotherm Ninhydrin assay
Nanobeacon diameter	300 – 350 nm	SEM, DLS
FL intensity[a]	300,000[b]	Fluorometer
Coumarin 6 per nanoparticle	0.05 wt%	UV-Vis

Table 2

Ratio-imaging index F_{ROI}/F_0 of the nanobeacon tested on an orthotopic rat model of CRC (n = 6) at a concentration of 2 mg/mL.

Ratio Imaging Fluorescence			
	Mean Fluorescence	**P values**	**F_{ROI}/F_0**
Splenic flexure	131.7 ± 0.08	< 0.001	1.3
Tumor	170.1 ± 0.2	< 0.005	